

Implications of Protonation and Substituent Effects for C–O and O–P Bond Cleavage in Phosphate Monoesters

Paul G. Loncke[†] and Paul J. Berti^{*†‡}

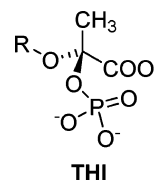
Contribution from the Department of Chemistry, Department of Biochemistry and Biomedical Sciences, McMaster University, 1280 Main Street West, Hamilton, ON, L8S 4M1, Canada

Received October 31, 2005; E-mail: berti@mcmaster.ca

Abstract: A recent study of phosphate monoesters that broke down exclusively through C–O bond cleavage and whose reactivity was unaffected by protonation of the nonbridging oxygens (Byczynski et al. *J. Am. Chem. Soc.* **2003**, *125*, 12541) raised several questions about the reactivity of phosphate monoesters, R–O–P_i. Potential catalytic strategies, particularly with regard to selectively promoting C–O or O–P bond cleavage, were investigated computationally through simple alkyl and aryl phosphate monoesters. Both C–O and O–P bonds lengthened upon protonating the bridging oxygen, R–O(H⁺)–P_i, and heterolytic bond dissociation energies, ΔH_{C-O} and ΔH_{O-P} , decreased. Which bond will break depends on the protonation state of the phosphoryl moiety, P_i, and the identity of the organosubstituent, R. Protonating the bridging oxygen when the nonbridging oxygens were already protonated favored C–O cleavage, while protonating the bridging oxygen of the dianion form, R–O–PO₃²⁻, favored O–P cleavage. Alkyl R groups capable of forming stable cations were more prone to C–O bond cleavage, with *t*Bu > *i*Pr > F₂*i*Pr > Me. The lack of effect on the C–O cleavage rate from protonating nonbridging oxygens could arise from two precisely offsetting effects: Protonating nonbridging oxygens lengthens the C–O bond, making it more reactive, but also decreases the bridging oxygen proton affinity, making it less likely to be protonated and, therefore, less reactive. The lack of effect could also arise without bridging oxygen protonation if the ratio of rate constants with different protonation states precisely matched the ratio of acidity constants, *K*_a. Calculations used hybrid density functional theory (B3PW91/6-31++G**) methods with a conductor-like polarizable continuum model (CPCM) of solvation. Calculations on Me-phosphate using MP2/aug-cc-pVDZ and PBE0/aug-cc-pVDZ levels of theory, and variations on the solvation model, confirmed the reproducibility with different computational models.

Phosphate monoesters have long been studied due to both their biological importance and their interesting reactivity.^{1–13} Aryl and most primary alkyl phosphate monoesters are hydrolyzed exclusively or predominantly through O–P bond cleavage, though primary alkyl phosphate monoesters show some C–O cleavage in strong acid.^{1,6,14–17} At the opposite extreme, the

tetrahedral intermediates (THI)¹⁸ formed by the enzymes AroA and MurA underwent nonenzymatic breakdown exclusively through C–O bond cleavage, even at pH > 10.¹⁹ Other phosphate monoesters show intermediate behaviors, with varying proportions of C–O and O–P bond cleavage, but always with more C–O cleavage at lower pH and more O–P bond cleavage at higher pH.^{15,20–25}



O–P cleavage has been shown by a variety of techniques to proceed through highly dissociative A_ND_N²⁶ (S_N2) transition

[†] Department of Chemistry.

[‡] Department of Biochemistry and Biomedical Sciences.

- (1) Cox, J. R., Jr.; Ramsay, O. B. *Chem. Rev.* **1964**, *64*, 317–352.
- (2) Thatcher, G. R. J.; Kluger, R. *Adv. Phys. Org. Chem.* **1989**, *25*, 99–265.
- (3) Hengge, A. C. In *Comprehensive Biological Catalysis*; Sinnott, M., Ed. Academic Press: London, 1998; pp 517–542.
- (4) Hengge, A. C. *Acc. Chem. Res.* **2002**, *35*, 105–112.
- (5) Lad, C.; Williams, N. H.; Wolfenden, R. *Proc. Natl. Acad. Sci. U.S.A.* **2003**, *100*, 5607–5610.
- (6) Wolfenden, R.; Ridgway, C.; Young, G. *J. Am. Chem. Soc.* **1998**, *120*, 833–834.
- (7) Kirby, A. J.; Dutta-Roy, N.; da Silva, D.; Goodman, J. M.; Lima, M. F.; Roussev, C. D.; Nome, F. *J. Am. Chem. Soc.* **2005**, *127*, 7033–7040.
- (8) Yang, M. Y.; Iranzo, O.; Richard, J. P.; Morrow, J. R. *J. Am. Chem. Soc.* **2005**, *127*, 1064–1065.
- (9) O'Brien, P. J.; Herschlag, D. *Biochemistry* **2002**, *41*, 3207–3225.
- (10) Nikolic-Hughes, I.; Rees, D. C.; Herschlag, D. *J. Am. Chem. Soc.* **2004**, *126*, 11814–11819.
- (11) Range, K.; McGrath, M. J.; Lopez, X.; York, D. M. *J. Am. Chem. Soc.* **2004**, *126*, 1654–1665.
- (12) Wolfenden, R.; Zhao, F. *J. Am. Chem. Soc.* **2004**, *126*, 8646–8647.
- (13) Cheng, Y. H.; Zhang, Y. K.; McCammon, J. A. *J. Am. Chem. Soc.* **2005**, *127*, 1553–1562.
- (14) Bunton, C. A.; Llewellyn, D. R.; Oldham, K. G.; Vernon, C. A. *J. Chem. Soc.* **1958**, 3574–3587.

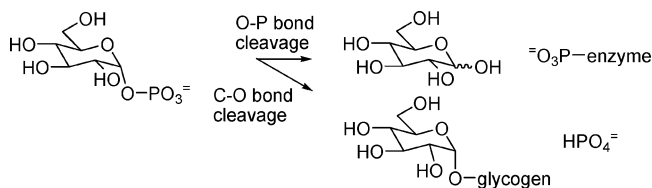
- (15) Kugel, L.; Halmann, M. *J. Org. Chem.* **1967**, *32*, 642–647.
- (16) Kirby, A. J.; Varvoglis, G. A. *J. Am. Chem. Soc.* **1967**, *89*, 415–423.
- (17) Barnard, P. W. C.; Bunton, C. A.; Kellerman, D.; Mhala, M. M.; Silver, B.; Vernon, C. A.; Welch, V. A. *J. Chem. Soc. B* **1966**, 227–235.
- (18) Abbreviations: ΔH_{C-O} , ΔH_{O-P} , heterolytic bond dissociation energies of C–O and O–P bonds; AIM, atoms-in-molecules theory; CPCM, conductor-like polarizable continuum solvation model; DFT, density functional theory, PA, proton affinity; P_i, PO₃H_nⁿ⁻² (n = 0–3); THI, tetrahedral intermediate.
- (19) Byczynski, B.; Mizyed, S.; Berti, P. J. *J. Am. Chem. Soc.* **2003**, *125*, 12541–12550.

states in a variety of enzymatic^{9,10,27–34} and nonenzymatic reactions,^{7,16,35,36} with little nucleophile participation at the transition state.^{2,3,7,16,37–39} That is, O–P bond breakage is far advanced over P–Nucleophile bond formation, and the transition state is highly metaphosphate (PO_3^-)-like. The catalytic effect of protonating the bridging oxygen is well recognized. There is evidence for a discrete metaphosphate intermediate in some reactions in organic solvents,² and an enzyme-bound metaphosphate was reported in the crystal structure of fructose 1,6-bisphosphate.⁴⁰ It is relatively stable in the gas phase,⁴¹ but metaphosphate is generally considered too unstable to exist in protic solvents. Recent computational studies have addressed O–P bond cleavage and metaphosphate reactivity in solution.^{11,42–45} C–O cleavage in phosphate monoesters has been widely observed but, with a few exceptions,^{15,19,23–25,46,47} has not been characterized in detail.

The potential effectiveness of acid catalysis is difficult to assess exactly because the unprotonated forms are so unreactive. O–P hydrolysis is specific acid-catalyzed even in 1 M KOH, implying a $>10^8$ -fold effect upon protonation of the dianion form.^{5,6} A recent study on intramolecular general acid catalysis of O–P bond cleavage showed a similar rate acceleration.⁷ Similarly, C–O cleavage in THI breakdown was acid-catalyzed to at least pH 12, indicating a $>10^7$ -fold effect from protonation.¹⁹

The mechanistic imperative for enzymes catalyzing phosphate hydrolyses or transfers is not only to accelerate the reaction but also to ensure that the correct bond is cleaved. For example,

Scheme 1



phosphoglucosyltransferase cleaves the O–P bond in glucose 1-phosphate,^{48,49} while glycogen phosphorylase catalyzes C–O bond cleavage^{50–52} (Scheme 1). Alkaline phosphatase cleaves O–P bonds in a variety of substrates, including those prone to C–O bond cleavage.^{9,10,33}

Our interest in phosphate reactivity stems from recent studies on the THIs, α -carboxyketal phosphates formed in AroA- and MurA-catalyzed reactions.^{19,53} Nonenzymatic THI breakdown was facile, acid-catalyzed through protonation of the bridging oxygen and proceeded exclusively through C–O bond cleavage.¹⁹ In the enzymatic reactions, phosphate is eliminated to yield an *enol*pyruvyl product. AroA-catalyzed THI breakdown appears to proceed through a stepwise (E1) or highly dissociative mechanism, with phosphate departure (C–O cleavage) leading to deprotonation.⁵⁴ Surprisingly, neither protonation of the non-bridging phosphate oxygens nor interactions with cationic side chains had measurable effects on C–O bond cleavage.

Those studies raised several fundamental questions about phosphate monoester chemistry: Why does nonbridging oxygen protonation not affect the rate of THI breakdown? What catalytic strategies are effective for C–O and O–P cleavage? What factors control the choice between C–O and O–P cleavage, and how do enzymes influence that? In this study we have examined the reactivity of simple phosphate monoesters as a function of protonation state, protonation site, and organosubstituents in order to better understand the criteria for C–O versus O–P bond cleavage and to identify what catalytic strategies are likely to be effective in phosphate monoester chemistry.

Methods

The geometries of six phosphate monoesters in all possible protonation states were determined, as well as the products of heterolytic bond dissociation for the alkyl phosphate monoesters using the Gaussian 03 suite of programs (Figure 1).⁵⁵ All geometries were fully optimized and confirmed as minima by numerical frequency analysis, except $\text{F}_2\text{iPr}-\text{O}(\text{H}^+)-\text{PO}_3\text{H}_3^+$, which had a small imaginary frequency, $28i\text{ cm}^{-1}$, in the optimized structure, corresponding to a dihedral angle rotation. Numerical frequencies were used because analytical frequency calculations often resulted in small negative eigenvalues, most likely

- (20) Kumamoto, J.; Westheimer, F. H. *J. Am. Chem. Soc.* **1955**, *77*, 2515–2518.
 (21) Parente, J. E.; Rislely, J. M.; Van Etten, R. L. *J. Am. Chem. Soc.* **1984**, *106*, 8156–8161.
 (22) Butcher, W. W.; Westheimer, F. H. *J. Am. Chem. Soc.* **1955**, *77*, 2420–2424.
 (23) Lapidot, A.; Samuel, D.; Weiss-Brodsky, M. *J. Chem. Soc.* **1964**, 637–643.
 (24) Bunton, C. A.; Hummer, E. *J. Org. Chem.* **1969**, *34*, 572–576.
 (25) Bunton, C. A.; Llewellyn, D. R.; Oldham, K. G.; Vernon, C. A. *J. Chem. Soc.* **1958**, 3588–3594.
 (26) According to IUPAC nomenclature, a mechanism is divided into elementary steps, with A_N representing nucleophilic addition and D_N representing nucleophilic dissociation. A bimolecular ($\text{S}_\text{N}2$) reaction is $\text{A}_\text{N}\text{D}_\text{N}$. $\text{D}_\text{N}^*\text{A}_\text{N}$ and $\text{D}_\text{N}+\text{A}_\text{N}$ mechanisms are stepwise ($\text{S}_\text{N}1$), with a discrete intermediate. “*” or “+” denotes an intermediate too short-lived for the leaving group to diffuse into solution or one that is long-lived enough to diffusively equilibrate with solvent, respectively. (Guthrie, R. D.; Jencks, W. P. *Acc. Chem. Res.* **1989**, *22*, 343–349.)
 (27) Hengge, A. C.; Zhao, Y.; Wu, L.; Zhang, Z. Y. *Biochemistry* **1997**, *36*, 7928–7936.
 (28) Hengge, A. C.; Martin, B. L. *Biochemistry* **1997**, *36*, 10185–10191.
 (29) Rawlings, J.; Hengge, A. C.; Cleland, W. W. *J. Am. Chem. Soc.* **1997**, *119*, 542–549.
 (30) Hoff, R. H.; Mertz, P.; Rusnak, F.; Hengge, A. C. *J. Am. Chem. Soc.* **1999**, *121*, 6382–6390.
 (31) Hoff, R. H.; Wu, L.; Zhou, B.; Zhang, Z. Y.; Hengge, A. C. *J. Am. Chem. Soc.* **1999**, *121*, 9514–9521.
 (32) McCain, D. F.; Grzyzka, P. K.; Wu, L.; Hengge, A. C.; Zhang, Z. Y. *Biochemistry* **2004**, *43*, 8256–8264.
 (33) O’Brien, P. J.; Herschlag, D. *J. Am. Chem. Soc.* **1999**, *121*, 11022–11023.
 (34) Hengge, A. C.; Sowa, G. A.; Wu, L.; Zhang, Z. Y. *Biochemistry* **1995**, *34*, 13982–13987.
 (35) Hengge, A. C.; Edens, W. A.; Elsing, H. *J. Am. Chem. Soc.* **1994**, *116*, 5045–5049.
 (36) Hengge, A. C.; Hess, R. A. *J. Am. Chem. Soc.* **1994**, *116*, 11256–11263.
 (37) Herschlag, D.; Jencks, W. P. *J. Am. Chem. Soc.* **1987**, *109*, 4665–4674.
 (38) Kirby, A. J.; Lima, M. F.; da Silva, D.; Nome, F. *J. Am. Chem. Soc.* **2004**, *126*, 1350–1351.
 (39) Kirby, A. J.; Varvoglis, G. A. *J. Chem. Soc. B* **1968**, 135–141.
 (40) Choe, J. Y.; Iancu, C. V.; Fromm, H. J.; Honzatko, R. B. *J. Biol. Chem.* **2003**, *278*, 16015–16020.
 (41) Henchman, M.; Viggiano, A. A.; Paulson, J. F.; Freedman, A.; Wormhoudt, J. *J. Am. Chem. Soc.* **1985**, *107*, 1453–1455.
 (42) Hu, C.-H.; Brinck, T. *J. Phys. Chem. A* **1999**, *103*, 5379–5386.
 (43) Bianciotto, M.; Barthelat, J.-C.; Vigroux, A. *J. Phys. Chem. A* **2002**, *106*, 6521–6526.
 (44) Bianciotto, M.; Barthelat, J.-C.; Vigroux, A. *J. Am. Chem. Soc.* **2002**, *124*, 7573–7587.

- (45) Zhang, L. D.; Xie, D. Q.; Xu, D. G.; Guo, H. *J. Phys. Chem. A* **2005**, *109*, 11295–11303.
 (46) Withers, S. G.; Percival, M. D.; Street, I. P. *Carbohydr. Res.* **1989**, *187*, 43–66.
 (47) Withers, S. G.; MacLennan, D. J.; Street, I. P. *Carbohydr. Res.* **1986**, *154*, 127–144.
 (48) Lahiri, S. D.; Zhang, G.; Dunaway-Mariano, D.; Allen, K. N. *Biochemistry* **2002**, *41*, 8351–8359.
 (49) Ray, W. J., Jr.; Puvathingal, J. M. *Biochemistry* **1990**, *29*, 2790–2801.
 (50) Johnson, L. N.; Hu, S. H.; Barford, D. *Faraday Discuss.* **1992**, 131–142.
 (51) Chrysin, E. D.; Kosmopoulou, M. N.; Tiraidis, C.; Kardakaris, R.; Bischler, N.; Leonidas, D. D.; Hadady, Z.; Somsak, L.; Docsa, T.; Gergely, P.; Oikonomakos, N. G. *Protein Sci.* **2005**, *14*, 873–888.
 (52) Mitchell, E. P.; Withers, S. G.; Ermert, P.; Vasella, A. T.; Garman, E. F.; Oikonomakos, N. G.; Johnson, L. N. *Biochemistry* **1996**, *35*, 7341–7355.
 (53) Mizyed, S.; Wright, J. E. I.; Byczynski, B.; Berti, P. J. *Biochemistry* **2003**, *42*, 6986–6995.
 (54) Clark, M. E.; Berti, P. J. Submitted for publication.
 (55) Frisch et al. *Gaussian 03*; Gaussian, Inc.: Wallingford, CT, 2004.

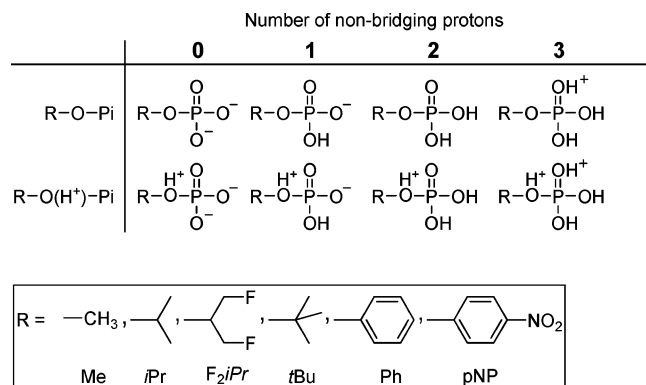


Figure 1. Structures and protonation states of molecules investigated.

due to the fact that second derivatives are not fully analytic in the solvation model.⁵⁶

The default method for this study was the hybrid Becke three-parameter Perdew–Wang 1991 (B3PW91) density-functional theory (DFT) method^{57,58} with the standard 6-31++G** basis set and water solvation simulated by the Conductor-like Polarizable Continuum Model (CPCM).^{56,59} The solute cavity in the CPCM calculations, created from interlocking atomic spheres according to the generating polyhedra (GEPOL) procedure,⁶⁰ was built using the default United Atom Topology Model⁶¹ with atomic radii from the UFF force field (RADII = UA0). In the UA0 topology model, hydrogen atoms are included in the spheres of the heavy atoms to which they are bonded, unless the heavy atoms are strongly electronegative, in which case hydrogens are assigned individual spheres. Radii for extra spheres added to smooth the cavity were set to have a minimum value of 0.5 Å (RMIN = 0.5), the overlap index between interlocking spheres was set to 0.8 (OFAC = 0.8), and the continuum dielectric constant was $\epsilon = 78$, equal to water's.

The computational method and solvation model were validated with additional calculations on the Me-phosphate series to confirm that the structural and energetic trends observed were not sensitive to model chemistry and radii used for the solvation model. The DFT method was tested by performing calculations with the same solvation model at the MP2/aug-cc-pVDZ level of theory, that is, second-order Møller–Plesset theory with Dunning's correlation consistent aug-cc-pVDZ basis set. The solvation model was varied with the default DFT method by using explicit hydrogens included for every heavy atom (RADII=UFF). Finally, the Perdew–Burke–Ernzerhof generalized gradient approximation DFT method, i.e., PBE0/aug-cc-pVDZ, was used with the CPCM solute cavity calculated using Pauling atomic radii (RADII=Pauling), which gave a solute cavity with a 45% smaller volume than the UFF method.

Heterolytic bond dissociation energies, ΔH , were calculated as follows: $\Delta H_{C-O}(R-O-P_i)$ was for $R-O-P_i \rightleftharpoons \{R^+ + ^-O-P_i\}$; $\Delta H_{C-O}(R-O(H^+)-P_i)$ was for $R-O(H^+)-P_i \rightleftharpoons \{R^+ + HO-P_i\}$; $\Delta H_{O-P}(R-O-P_i)$ was for $R-O-P_i \rightleftharpoons \{R-O^- + PO_3H_n^{n-1}\}$; and $\Delta H_{O-P}(R-O(H^+)-P_i)$ was for $R-O(H^+)-P_i \rightleftharpoons \{R-OH + PO_3H_n^{n-1}\}$. Molecular structure analyses and atomic charge calculations were based on the quantum theory of atoms in molecules⁶² (QT-AIM) using the AIMPAC suite of programs⁶³ and AIM2000, version 1.⁶⁴ Charges were

also calculated using the Mulliken, Natural Population Analysis (NPA) and Charges from Electrostatic Potential, Grid Method (CHELPG) methods.⁶⁵

Results

Geometries were optimized for all the possible protonation states of the phosphate monoesters, $R-O-P_i$, plus the same species with a protonated bridging oxygen, $R-O(H^+)-P_i$ at the B3PW91/6-31++G** level of theory with a CPCM model of solvation with atomic radii calculated using the united atom approach (UA0) (Figures 2 and 3, and Supporting Information, Figure S1, Table S1). Other computational methods were tested with Me-phosphate. They gave similar structures and energies and the same structural and energetic trends in response to protonation (Figure S2, Tables S2, S3). The methods tested included second-order Møller–Plesset theory, MP2/aug-cc-pVDZ with our default solvation model, the Perdew–Burke–Ernzerhof DFT method, i.e., PBE0/aug-cc-pVDZ, with the solute cavity calculated using Pauling radii, and our default B3PW91/6-31++G** DFT method with the solute cavity calculated using UFF radii with explicit hydrogen atoms.

The consistency of DFT and MP2 results lends support to the correctness of the computational model because when these methods fail, it tends to be for different reasons. DFT usually gives excellent results for molecular dissociation and is reliable for predicting the electronic structure of anions^{66,67} but can fail in describing the delocalized exchange-correlation hole, and thus overbind the electrons.^{68,69} The Møller–Plesset perturbation series can be problematic with anions because of a nonphysical “autoionization” phenomenon;⁷⁰ however this is seldom a problem at the MP2 level, and MP2 is commonly employed for molecular anions. The agreement between the MP2 and DFT results supports the reliability of our results.

A recent study demonstrated that a PCM continuum solvation model gave similar results to those including explicit waters for O–P hydrolysis of $Me-O(H^+)-PO_3^{2-}$.^{43,44} $Me-O(H^+)-PO_3^{2-}$ was a stable species with PCM or explicit water solvation, but the O–P bond spontaneously cleaved in gas-phase calculations. Similarly, in this study, $R-O(H^+)-PO_3^{2-}$ species were stable with CPCM continuum solvation (Figure 1), but the O–P bonds spontaneously cleaved in gas-phase calculations (data not shown). The $R-O(H^+)-PO_3H_3^+$ species were stable with CPCM solvation, but the C–O bonds spontaneously cleaved in the gas phase. Thus, the essential correctness of the solvation model was supported by: (i) its similarity to previously reported results,^{42–44} (ii) the insensitivity to different methods of calculating radii in the solute cavity (Figure S2), and (iii) the gas-phase calculations, which mirrored the trends with CPCM solvation, but with more extreme effects. These computational findings are consistent with experimental results^{7,16,41,71} that show that the O–P bond is more labile and metaphosphate, PO_3^- , is more stable in the gas phase and organic solvents than in water.

(56) Cossi, M.; Rega, N.; Scalmani, G.; Barone, V. *J. Comput. Chem.* **2003**, *24*, 669–681.

(57) Perdew, J. P.; Wang, Y. *Phys. Rev. B* **1992**, *45*, 13244.

(58) Becke, A. D. *J. Chem. Phys.* **1993**, *98*, 1372–1377.

(59) Barone, V.; Cossi, M. *J. Phys. Chem. A* **1998**, *102*, 1995–2001.

(60) Pascualhuir, J. L.; Silla, E.; Tunon, I. *J. Comput. Chem.* **1994**, *15*, 1127–1138.

(61) Barone, V.; Cossi, M.; Tomasi, J. *J. Chem. Phys.* **1997**, *107*, 3210–3221.

(62) Bader, R. F. W. *Atoms in Molecules. A Quantum Theory*; Clarendon Press: Oxford, 1990.

(63) Biegler-Koenig, F. W.; Bader, R. F. W.; Tang, T. H. *J. Comput. Chem.* **1982**, *3*, 317–328.

(64) Biegler-Koenig, F. W.; Schonbohm, J.; Bayles, D. *J. Comput. Chem.* **2001**, *22*, 545–559.

(65) Breneman, C. M.; Wiberg, K. B. *J. Comput. Chem.* **1990**, *11*, 361–373.

(66) Galbraith, J. M.; Schaefer, H. F. *J. Chem. Phys.* **1996**, *105*, 862–864.

(67) Tschumper, G. S.; Schaefer, H. F. *J. Chem. Phys.* **1997**, *107*, 2529–2541.

(68) Gritsenko, O. V.; Ensing, B.; Schipper, P. R. T.; Baerends, E. J. *J. Phys. Chem. A* **2000**, *104*, 8558–8565.

(69) Ayers, P. W.; Yang, W. In *Computational Medicinal Chemistry for Drug Discovery*; Bultinck, P., de Winter, H., Langenaeker, W., Tollenaere, J. P., Eds.; Dekker: New York, 2003; pp 571–616.

(70) Stillinger, F. H. *J. Chem. Phys.* **2000**, *112*, 9711–9715.

(71) Cullis, P. M.; Rous, A. J. *J. Am. Chem. Soc.* **1986**, *108*, 1298–1300.

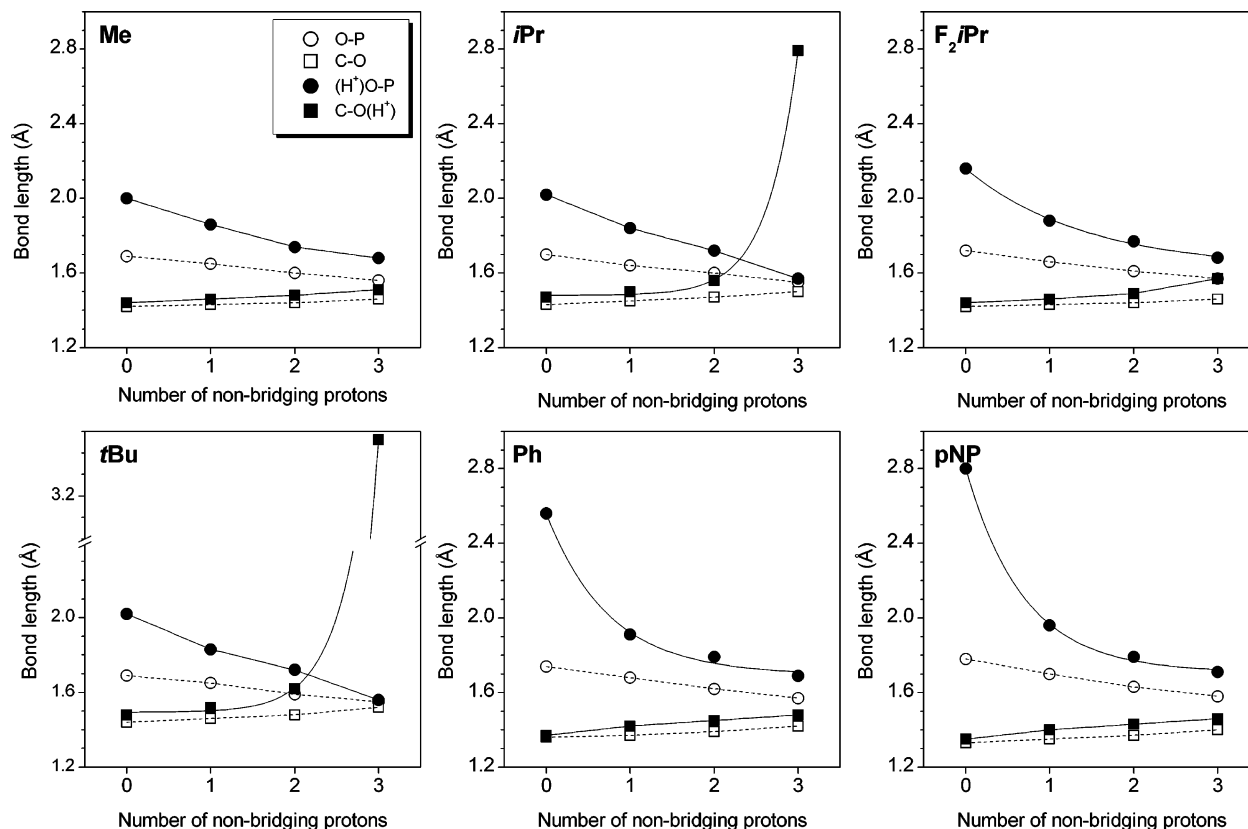


Figure 2. C–O and O–P bond lengths as a function of protonation state of nonbridging oxygens and organosubstituent. Bond lengths for R–O–P_i (open symbols, dashed lines) and R–O(H⁺)–P_i (solid symbols, solid lines) species are shown. The lines are meant as visual aids only.

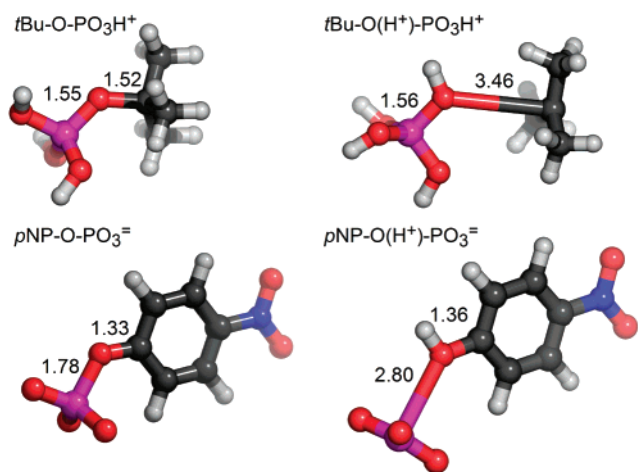


Figure 3. Structures which showed the largest effects upon protonating the bridging oxygens, *t*Bu–O–PO₃H⁺ and pNP–O–PO₃²⁻. O–P and C–O bond lengths are shown in angstroms.

Species triply protonated on the nonbridging oxygens are likely to form only in highly acidic conditions (e.g., >50% HClO₄)⁷² but were useful in this study to characterize changes under extreme conditions. Proton affinities (PAs) and heterolytic bond dissociation energies (ΔH_{C-O} , ΔH_{O-P}) were determined for selected structures (Figures 4 and 5, Table S4). Bond critical point electronic densities (Figure S3), $\rho_b(r)$,⁷³ which correlate with bond strength⁷⁴ and atomic charges (Figure S4) were

determined, and Me–O–P_i was optimized with a guanidinium ion replacing a proton (Figure S5).

Discussion

Structure and Dissociation Energy as Probes of Reactivity. Reactant (ground state) structures and heterolytic bond dissociation energies were used in this study as probes of reactivity. This approach is justified in terms of (i) longer bonds being more reactive and (ii) the transition states for the reactions of interest being very similar to the products of unimolecular dissociation.

(i) A specific experimental correlation was demonstrated between the reactivity of C–O and O–P bonds and their bond lengths in crystal structures of acetals and phosphate monoesters.^{75–78} For bond orders around unity, there was a linear relationship between the activation energy for unimolecular heterolysis and bond length, with a value of ~ 250 (kcal/mol)/Å for both C–O and O–P bonds.⁷⁷

(ii) The transition states for the reactions of interest will be similar to the products of unimolecular dissociation. In the cases where evidence exists, phosphate monoester hydrolysis through C–O bond cleavage proceeds through highly dissociative⁷⁹ mechanisms that tread the borderline between bimolecular A_ND_N²⁶ (S_N2) and unimolecular D_N*A_N (S_N1) transition states.^{19,46,47} O–P bond cleavage in aqueous solution is well-known to similarly proceed through highly dissociative, meta-

(72) Guthrie, J. P. *J. Am. Chem. Soc.* **1977**, *99*, 3991–4001.

(73) In AIM analyses, the bond critical point is the point of minimum electronic density along a bond (or bond path) and maximum electronic density in all other directions.

(74) O'Brien, S. E.; Popelier, P. L. A. *Can. J. Chem.* **1999**, *77*, 28–36.

(75) Allen, F. H.; Kirby, A. J. *J. Am. Chem. Soc.* **1984**, *106*, 6197–6200.

(76) Briggs, A. J.; Glenn, R.; Jones, P. G.; Kirby, A. J.; Ramaswamy, P. *J. Am. Chem. Soc.* **1984**, *106*, 6200–6206.

(77) Jones, P. G.; Kirby, A. J. *J. Am. Chem. Soc.* **1984**, *106*, 6207–6212.

(78) Deslongchamps, P.; Jones, P. G.; Li, S.; Kirby, A. J.; Kuusela, S.; Ma, Y. *J. Chem. Soc., Perkin Trans. 2* **1997**, 2621–2626.

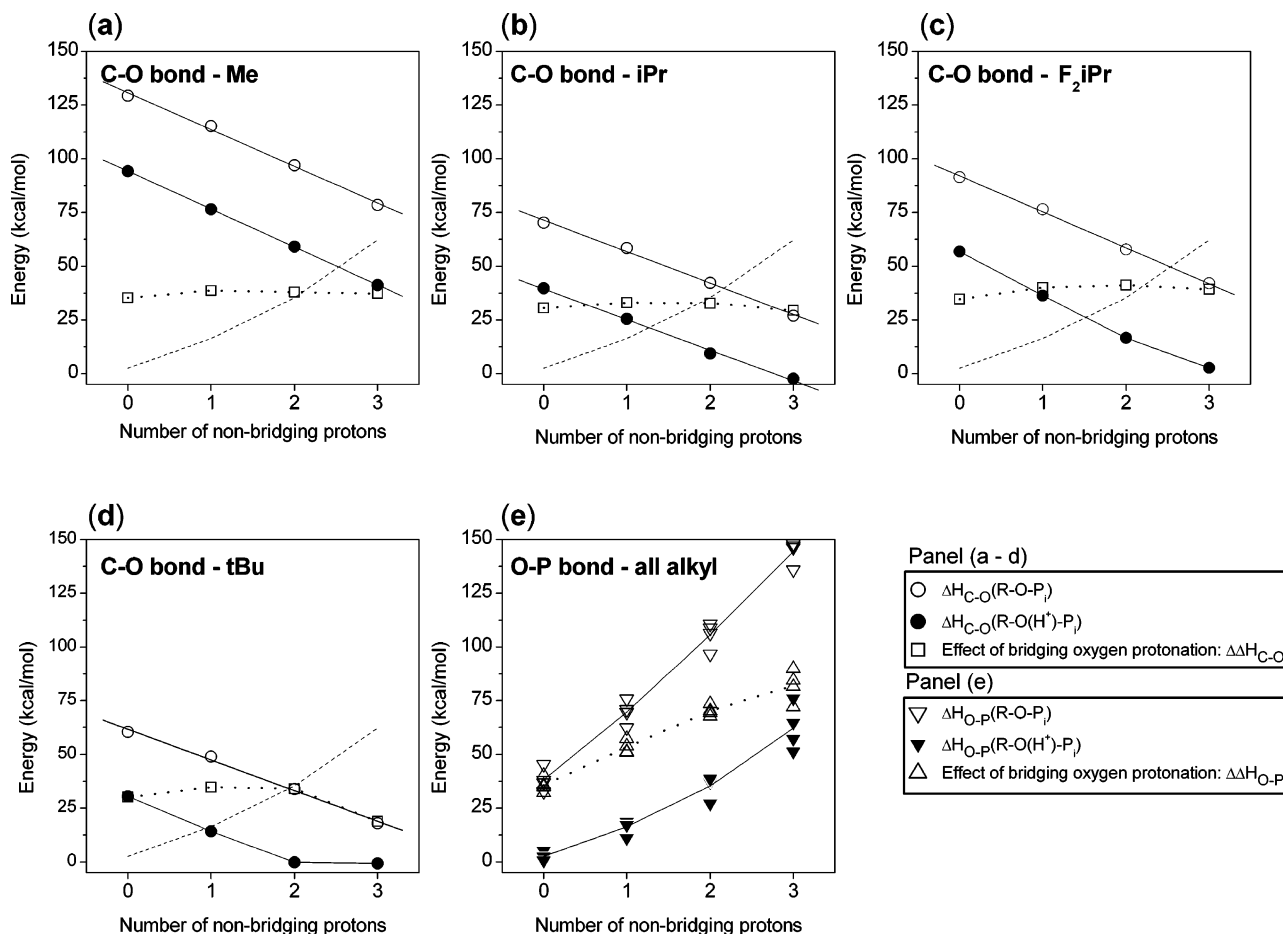


Figure 4. C–O and O–P heterolytic bond dissociation energies as a function of protonation state of nonbridging oxygens, and organosubstituent. (Panels a to d) ΔH_{C-O} for R–O–P_i and R–O(H⁺)–P_i species. Effect of bridging oxygen protonation was $\Delta\Delta H_{C-O} = \Delta H_{C-O}(R-O-P_i) - \Delta H_{C-O}(R-O(H^+)-P_i)$. For comparison, the dashed lines represent $\Delta H_{O-P}(R-O(H^+)-P_i)$. The lines are meant as visual aids only. (Panel e) O–P heterolytic bond dissociation energies for all alkyl phosphate monoester species, ΔH_{O-P} .

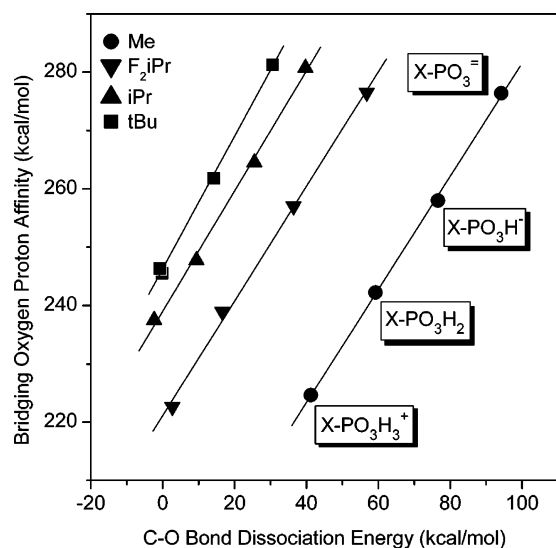


Figure 5. Correlation of bridging oxygen proton affinities (PAs) and C–O heterolytic bond dissociation energies, $\Delta H_{C-O}(R-O(H^+)-P_i)$. Bridging oxygen PAs were calculated for each protonation state of the nonbridging oxygens for Me–O(H⁺)–P_i, F₂iPr–O(H⁺)–P_i, iPr–O(H⁺)–P_i, and tBu–O(H⁺)–P_i.

phosphate-like $A_N D_N$ transition states.^{3,7,23} In each case, bond breakage is more advanced than bond formation, and the electrophile (carbocation or metaphosphate) has strong cationic character. Similarly, enzymatic O–P cleavage reactions for a

number of enzymes have been shown to be highly dissociative^{9,10,30,31,33,34} with little nucleophile participation, as reflected in very small β_{nuc} values.^{2,3,16,37} Recently, two crystal structures of fructose 1,6-bisphosphatase were reported to contain a discrete enzyme-bound metaphosphate intermediate in the active site.⁴⁰ With regards to C–O cleavage, phosphate elimination from the THI in the AroA-catalyzed reaction appears to proceed through a highly dissociative mechanism,⁵⁴ and the nonenzymatic reaction also appears to be stepwise, with phosphate departure preceding deprotonation of the cationic intermediate.¹⁹ In each case, the Hammond postulate requires that the transition state, whether concerted or stepwise, be structurally and energetically similar to the cationic species. Thus, in this study, anything that lengthens or shortens C–O or O–P bonds in the reactant is expected to have a corresponding effect on the rate of unimolecular heterolysis and, thus, on the overall reaction rate. By similar reasoning, heterolytic bond dissociation energies should accurately reflect reactivity trends.

(79) We use the word “dissociative” to indicate that the sum of nucleophile and leaving group bond orders at a transition state is less than the corresponding bond orders in the reactants or products. Thus, the loss of leaving group bond order is necessarily greater than the increase in bond order to the incoming nucleophile. In associative transition states, there is greater formation of bond order to the nucleophile than loss of bond order, while in synchronous transition states, bond making and breaking are equal to each other. (ref 9, and Berti, P. J. *Methods Enzymol.* **1999**, *308*, 355–397; Berti, P. J.; Tanaka, K. S. E. *Adv. Phys. Org. Chem.* **2002**, *37*, 239–314.)

General Trends. The effects of both protonation and organosubstituents were visible in both the structures and heterolytic bond dissociation energies, ΔH (Figures 2–4). Two clear trends emerged: Protonation of nonbridging oxygens caused C–O bonds to lengthen and ΔH_{C-O} 's to decrease, while O–P bonds shortened and ΔH_{O-P} 's increased. Protonation of bridging oxygens caused both C–O and O–P bonds to lengthen and both ΔH_{C-O} 's and ΔH_{O-P} 's to decrease. At the extremes, the O–P bond length in $pNP-O(H^+)-PO_3^{2-}$ was 2.8 Å, while, in $tBu-O(H^+)-PO_3H_3^+$, the C–O distance was 3.5 Å (Figure 3).⁸⁰ Bridging oxygen protonation would be catalytic for both C–O and O–P bond cleavage. The potential catalytic enhancement can be approximated from the difference in ΔH 's; that is, $\Delta\Delta H_{C-O} = \Delta H_{C-O}(R-O-P_i) - \Delta H_{C-O}(R-O(H^+)-P_i)$, and similarly for $\Delta\Delta H_{O-P}$. Although ΔH_{C-O} varied with organosubstituent (see below), $\Delta\Delta H_{C-O}$ was remarkably consistent across protonation states and organosubstituents, being ~ 35 kcal/mol (Figure 4). This number is unrealistically large, but it does demonstrate a significant potential catalytic effect upon bridging oxygen protonation. Different tautomeric forms give the same products upon C–O cleavage, e.g., $R-O-PO_3H_2$ and $R-O(H^+)-PO_3H^-$ give R^+ and $H_2PO_4^-$. Thus, the differences in ΔH_{C-O} reflect differences in the reactant energies. In enzymatic reactions, protonation of the bridging oxygen in the reactant state will correspond to ground-state destabilization.

Both $\Delta H_{O-P}(R-O-P_i)$ and $\Delta H_{O-P}(R-O(H^+)-P_i)$ increased with protonation of nonbridging oxygens. There was little difference between alkyl organosubstituents. The potential catalytic effect of protonating the bridging oxygens, $\Delta\Delta H_{O-P}$, was large, >36 kcal/mol, and increased with the number of nonbridging protons (Figure 4e). However, the rapidly increasing values of ΔH_{O-P} and decreasing PA of the bridging oxygens (Figure 5) would disfavor O–P bond cleavage in highly protonated forms.

Protonation Effects. A. C–O Bond Cleavage. One of the motivations for this study was to understand the unexpected lack of effect of protonation of the nonbridging oxygens on acid-catalyzed THI breakdown (Figure 6).¹⁹ Similarly, the $\log(k)$ versus pH profiles for tBu ²³ and ribose 1-phosphate²⁴ are linear in the pH ranges where nonbridging oxygens are protonated, also indicating a lack of effect from protonation. Phosphate monoesters typically have pK_{a1} 's of 0.7 to 1.4 and pK_{a2} 's of 5.7 to 6.8.^{81–84}

Our results show that protonation of the nonbridging oxygens *does* affect both structure and heterolytic bond dissociation energies. There are two possible explanations for the lack of effect on reactivity of protonating nonbridging oxygens, both of which involve a coincidence of effects on pK_a and rate.

The first is that protonating the nonbridging oxygens makes the C–O bond more labile but also makes the bridging oxygen less basic and therefore less likely to be protonated. If these effects precisely balance each other, the result will be an apparent lack of effect upon protonation. This was tested by

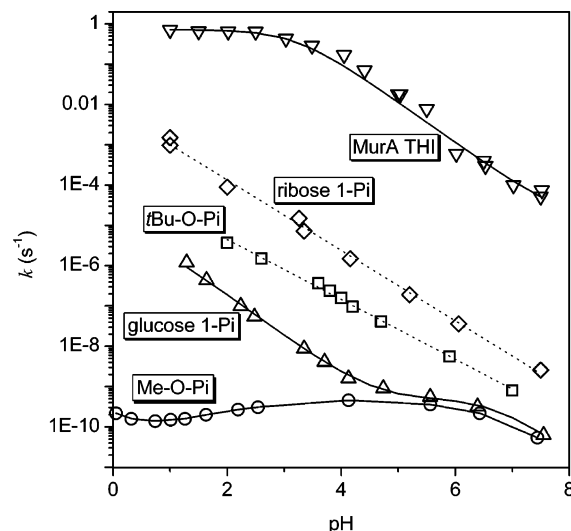


Figure 6. pH-dependencies of phosphate monoester breakdown in methyl-,¹⁴ glucose 1-,²⁵ tBu -,²³ and ribose 1-phosphates,²⁴ plus MurA THI,¹⁹ extrapolated to 25 °C. The plateau at pH < 4 in the MurA THI profile is from protonation of the adjacent α -carboxylate.

comparing ΔH_{C-O} 's and PAs. PAs correlate closely with relative pK_a 's for a variety of functional groups, including phosphates.^{11,85} Plots of bridging oxygen PAs versus ΔH_{C-O} showed linear correlations with slopes of unity (0.97 to 1.13) (Figure 5). This linear relationship supports offsetting effects on pK_a and reactivity, implying that the $\log(k)$ versus pH profile will be linear, as observed experimentally. The second explanation involves a coincidence between ΔpK_a and rate constants.^{86–88} The difference between pK_{a1} and pK_{a2} , typically ~ 5 pH units, means that $K_{a1}/K_{a2} = 10^5$. If the ratio of rate constants for $R-O-PO_3H_2$ versus $R-O-PO_3H^-$ is also 10^5 , then the pH profile will also be linear. This explanation does not require protonation of the bridging oxygen.

Both explanations require precisely matched effects on equilibrium and rate constants, which may seem unlikely at first glance; however: (i) deprotonation and C–O bond cleavage are very similar reactions, both involving dissociation of a cation from an oxygen atom, (ii) various fits to experimental data show that the pH dependence would appear linear within experimental error even if the offsetting factors differed by a factor of ~ 5 , and (iii) this same effect is observed with successive protonations of ring nitrogens in acid-catalyzed purine nucleoside hydrolysis.^{86,87}

An important consequence for enzymatic catalysis is that protonating nonbridging oxygens can be used to select for C–O over O–P bond cleavage.

B. C–O Bond Cleavage from $R-O-P_i$ Species? We favor C–O bond cleavage through protonation of the bridging oxygen; however, it would also be consistent with the existing kinetic data for phosphate hydrolysis to occur without protonation of the bridging oxygen, i.e., through $R-O-P_i$. The two tautomers of $R-(PO_4H_2)$, i.e., $R-O(H^+)-PO_3H^-$ and $R-O-PO_3H_2$, are kinetically equivalent, and rate data will not distinguish between them. ΔH_{C-O} decreases with each successive protonation of

(80) AIM analysis indicates there is a bond path between C and O. That is, there is formally a bond, though this species could more reasonably be considered as simply an ion complex.

(81) Hartman, F. C.; LaMuraglia, G. M.; Tomozawa, Y.; Wolfenden, R. *Biochemistry* **1975**, *14*, 5274–5279.

(82) O'Connor, J. V.; Barker, R. *Carbohydr. Res.* **1979**, *73*, 227–234.

(83) Massoud, S. S.; Sigel, H. *Inorg. Chem.* **1988**, *27*, 1447–1453.

(84) Saha, A.; Saha, N.; Ji, L.-n.; Zhao, J.; Gregan, F.; Sajadi, S. A. A.; Song, B.; Sigel, H. *J. Biol. Inorg. Chem.* **1996**, *1*, 231–238.

(85) Range, K.; Riccardi, D.; Cui, Q.; Elstner, M.; York, D. M. *Phys. Chem. Chem. Phys.* **2005**, *7*, 3070–3079.

(86) Zoltewicz, J. A.; Clark, D. F.; Sharpless, T. W.; Grahe, G. *J. Am. Chem. Soc.* **1970**, *92*, 1741–1749.

(87) Lindahl, T.; Nyberg, B. *Biochemistry* **1972**, *11*, 3610–3618.

(88) Berti, P. J.; McCann, J. A. *Chem. Rev.* **2006**, *106*, 506–555.

nonbridging oxygens (Figure 4), which would also be consistent with reaction through R–O–P_i. However, there is some reason to believe that C–O cleavage proceeds through bridging oxygen protonation, and in any event, the results presented here would not be greatly affected if nonenzymatic reactions did proceed through R–O–P_i. Evidence for bridging oxygen protonation includes the following: (i) Me-phosphate hydrolyzes through a mixture of C–O and O–P cleavage in strong acid, reported to be 73% C–O cleavage in both 4 M¹⁵ or 5 M¹⁴ HClO₄. According to our results, Me-phosphate would break down exclusively through O–P cleavage at all pH's if it proceeds through R–O–P_i (Figure 4). (ii) The catalytic advantage to C–O bond cleavage of protonating the bridging oxygen, $\Delta\Delta H_{C-O} \sim 35$ kcal/mol, is very large. (iii) A survey of enzyme X-ray crystal structures reveals that most or all position potential acid catalysts near the bridging oxygens (see below). (iv) The catalytic effect of protonating a single nonbridging oxygen in R–O–PO₃²⁻ would be modest; it would require protonating two nonbridging oxygens to give a significant effect.

If we assume that C–O hydrolyses do proceed through the R–O–P_i form, most of the conclusions of this study still hold, namely that for a given organosubstituent more highly protonated forms are more prone to C–O than O–P cleavage, that organosubstituents giving more stable cations are more prone to C–O bond cleavage, and that bridging oxygen protonation promotes both C–O and O–P bond cleavage.

C. O–P Bond Cleavage. The observed geometries and ΔH_{O-P} 's were consistent with the pH-dependence of O–P bond cleavage, which has a broad maximum around pH 4, corresponding to the monoanion form.^{2,3,7,14,43,44} The prevailing model of O–P bond cleavage involves proton transfer from the nonbridging to the bridging oxygen, yielding R–O(H⁺)–PO₃²⁻, the protonation state in this study with the longest O–P bonds and lowest ΔH_{O-P} 's. Previous computational studies have demonstrated the importance of Me–O(H⁺)–PO₃²⁻ as a key intermediate in Me-phosphate hydrolysis.^{43,44} In the dianion form, there is no proton to transfer, and in the neutral form, the bridging oxygen PA is lower and the O–P bond is stronger. Both effects decrease reactivity.

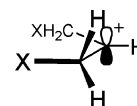
Organosubstituent Effects. The second major factor in determining reactivity was the identity of the organosubstituent. The effects on O–P bond reactivity were small, but C–O bonds were strongly affected by the organosubstituent, which therefore also affected the balance between C–O and O–P cleavage.

A. O–P Bonds. O–P bonds were largely unaffected by the identity of the alkyl substituents, consistent with solution studies of phosphate monoester structures by ³¹P NMR.⁸⁹ O–P bond lengths in the R–O–P_i forms of the Ph- and pNP-phosphates were similar to each other and similar to the alkyl phosphate monoesters. Bridging oxygen protonation had a greater effect on O–P bond lengths in the aryl phosphates, indicating a greater propensity for O–P cleavage (Figure 2).

B. C–O Bonds. Alkyl R–O–P_i species had similar bond lengths and responded similarly to protonation of nonbridging oxygens, though differences in the intrinsic stabilities of the R⁺ carbocation products of C–O bond dissociation gave different ΔH_{C-O} 's, in the order Me > F₂iPr > iPr > tBu (Figure 4). R–O(H⁺)–P_i species responded differently to protonation of nonbridging oxygens, with greatly elongated C–O bonds for

iPr and tBu in the highly protonated forms. The values of ΔH_{C-O} were uniformly ~ 35 kcal/mol lower than those for R–O–P_i species (see above).

The potential contributions of inductive, steric, and hyperconjugative effects to phosphate monoester reactivity were examined by comparing different organosubstituents. Inductive effects would be reflected by the Hammett constant, σ_m , which would be ~ 0.06 – 0.09 for F₂iPr, compared with Ph, 0.06; Me, -0.07 ; and iPr/tBu, -0.10 .⁹⁰ Steric hindrance around the C–O–P bond would be Me < iPr \approx Ph \leq F₂iPr < tBu. Hyperconjugative stabilization of the cation products of C–O bond dissociation would be (Me \ll) iPr \approx F₂iPr < tBu. Hyperconjugation from the σ -bonds of adjacent C–H bonds to form π -bonding interactions will help stabilize the cationic center in the product cations of C–O bond cleavage and in phosphate monoesters where there are significant decreases in C–O bond order. Hyperconjugation is strongly angle dependent, being maximal when the C–H bond is eclipsed with the nascent p-orbital of the cationic carbon, and zero when they are normal to each other.⁹¹ The two F₂iPr⁺ structures found, with the F atoms syn (F–C–C⁺–H $\approx 0^\circ$) or anti (F–C–C⁺–H $\approx 180^\circ$) (1) to H₂ would be as effective as iPr⁺ in hyperconjugative stabilization, having four C–H bonds engaged in hyperconjugation. The iPr⁺ cation had 1 as the optimal conformer, also giving four hyperconjugating C–H bonds. tBu⁺ has six hyperconjugating C–H bonds, while Me⁺ has none.



1, X = F/H

The trend in C–O bond lengths was Ph < Me \approx F₂iPr < iPr < tBu. The shorter bond lengths with F₂iPr than iPr were the result of the inductive effect of the F atoms drawing electrons into the C–O bond. The fact that C–O bonds were shorter in Ph-phosphate despite similar σ_m values for F₂iPr and Ph indicates that factors in addition to inductive effects were important. The near identity of bond lengths between Me- and F₂iPr-phosphate thus indicates a balance between inductive and steric effects. The increased C–O bond length in the R–O(H⁺)–PO₃H₃⁺ form of F₂iPr- versus Me-phosphate likely indicates hyperconjugation becoming significant due to the C–F bonds adopting an anti conformation, similar to 1, allowing the C–O bond to lengthen. ΔH_{C-O} values for F₂iPr were between Me and iPr, reflecting the hyperconjugative stabilization of F₂iPr⁺ which is not possible in Me⁺, but the lower intrinsic stability of F₂iPr⁺ than iPr⁺, by 16 kcal/mol, due to the electron-withdrawing F atoms. Thus, there is evidence for all three factors, i.e., inductive, steric, and hyperconjugative effects affecting reactivity.

C. C–O versus O–P Bond Cleavage. The results presented here indicate that the experimentally observed balance between C–O and O–P bond cleavage in alkyl phosphate monoesters is controlled more by the rates of C–O cleavage rather than the (relatively constant) rates of O–P cleavage. For example, with Me-phosphate, ΔH_{C-O} was less than ΔH_{O-P} only for Me–

(90) Hansch, C.; Leo, A.; Taft, R. W. *Chem. Rev.* **1991**, *91*, 165–195.

(91) Sunko, D. E.; Szele, I.; Hehre, W. J. *J. Am. Chem. Soc.* **1977**, *99*, 5000–5004.

(89) Sorensen-Stowell, K.; Hengge, A. C. *J. Org. Chem.* **2005**, *70*, 4805–4809.

$O(H^+)–PO_3H_3^+$, consistent with 100% O–P cleavage at pH 4 and 27% in 4 M¹⁵ or 5 M¹⁴ HClO₄. In contrast, the much more reactive *t*Bu-phosphate (Figure 6) proceeded with 100% C–O bond cleavage at pH 0 and 25% at pH 7,²³ consistent with the much smaller value of ΔH_{C-O} , which was less than ΔH_{O-P} for two or three nonbridging protons and roughly equal for *t*Bu– $O(H^+)–PO_3H^-$. Similarly, ribose 1-phosphate hydrolysis is faster than glucose 1-phosphate, which shifts from C–O cleavage to O–P at pH > 4;^{24,25} and THI hydrolysis (C–O only) is fastest of all (Figure 6).¹⁹

Structural Effects. The reciprocal behavior of the C–O and O–P bonds as a function of nonbridging oxygen protonation, with one shortening as the other lengthened, is consistent with the bridging oxygen being a hard (nonpolarizable) atom. Thus, strengthening the O–P bond will weaken the C–O bond rather than increase the total bonding to oxygen. Bridging oxygen protonation lengthened the C–O and O–P bonds to compensate for the increased bonding to the oxygen through the proton.

Atomic charges probed the ionic contribution of the C–O and O–P bonds (see Supporting Information). The Coulombic energies (q_1q_2/r) for C–O bonds were small in all cases and either favorable or unfavorable, depending on the charge calculation method. The Coulombic energies of O–P bonds were favorable by all methods, indicating a significant ionic contribution to bonding. The absolute values varied with charge calculation method, as expected given their somewhat arbitrary nature. Nevertheless, the Coulombic energy varied little with bond order, and q_1q_2 , even less, regardless of charge calculation method, implying that the relative contribution of ionic interactions to the O–P bond is larger for long O–P bonds and that bonding becomes increasingly covalent with increasing bond orders. This was consistent with the linearly increasing electron density at the bond critical points in both C–O and O–P bonds at higher bond orders.

Implications for Enzymatic Catalysis: Protonation versus Ionic Interactions in O–P Cleavage. Protonating nonbridging oxygens would be anticatalytic to O–P bond cleavage. Protonating a nonbridging oxygen of Me– $O(H^+)–PO_3^{2-}$ increased the O–P bond order⁹² by 54%, from 0.28 to 0.43. However, a primarily ionic interaction with guanidinium had a smaller effect on the O–P bond order, causing it to increase by only 18% to 0.33. This is consistent with investigations of the role of Arg in alkaline phosphatase^{10,33} and protein tyrosine phosphatase³¹ which demonstrated by linear free energy relationships and isotope effects that while the Arg interaction with nonbridging oxygens was important to catalysis, it did not cause a more associative transition state (i.e., higher O–P bond order), a finding that contradicted a number of mechanistic proposals (see references in ref 10).

Implications for Enzymatic Catalysis: C–O Cleavage. The results of this study imply that protonating the bridging oxygen will be an effective catalytic strategy to promote C–O bond cleavage. The value of protonating nonbridging oxygens is less clear. Given a pK_{a2} of 6.3 for a typical phosphate monoester, protonating a nonbridging oxygen would have a modest 13-fold ($= 10^{7.4-6.3}$) catalytic effect at physiological pH. Protonating two nonbridging oxygens would be required to

cause a significant catalytic effect, $\sim 2 \times 10^6$ -fold, assuming a typical pK_{a1} of 1.

A. Interactions through Bridging Oxygens. A survey of X-ray crystallographic structures reveals that most or all of the C–O cleaving enzymes for which relevant structures could be found interact with the bridging oxygen through potential Brønsted or Lewis acids. (Arg was not considered as a potential general acid catalyst.) These enzymes include AroA and MurA, which place Lys22 in contact with the bridging oxygen of the THI (PDB codes: 1Q36, 1RF4, 1Q3G).^{93–96} The unusually low pK_a of AroA Lys22, 7.6, ensures that it can act as a general acid catalyst.⁹⁷ Similarly, 3-deoxy-D-manno-2-octulosonate 8-phosphate (KDO8P) synthase (PDB code: 1FWW) and 3-deoxy-D-arabinoheptulosonate-7-phosphate (DAH7P) synthase (PDB code: 1RZM) had a Lys residue positioned to protonate the bridging oxygen of phosphoenolpyruvate.^{98,99} Several residues in a sialic acid synthase, NeuB, namely Lys129, Glu234, Glu25, or Mn²⁺ could act as Brønsted or Lewis general acid catalysts to promote phosphate departure from the presumed hemiacetal phosphate intermediate, either directly or through water-mediated interactions (PDB code: 1XUZ).¹⁰⁰ Sucrose phosphorylase is believed to protonate the phosphate bridging oxygen using Glu232 in the {glucose 1-phosphate + fructose → sucrose + phosphate} direction.¹⁰¹ The structure of thiamin phosphate synthase was not clear-cut. There was a potential catalytic contact with a Mg²⁺-bound water molecule in the pyrophosphate ester-containing substrate analogue (PDB code: 1G4P), but different conformations with the pyrophosphate product made it unclear which interactions were catalytically relevant.¹⁰² Glycogen and maltodextrin phosphorylase catalyze C–O cleavage in the {glucose 1-phosphate + R–OH → glucosyl–O–R + phosphate} direction, where R–OH is glycogen or maltodextrin. The observed retention of anomeric configuration would normally imply a double displacement mechanism with an acyl-enzyme intermediate,¹⁰³ but no candidate nucleophile is apparent. In a recent study on maltodextrin phosphorylase, the enzyme cofactor pyridoxal 5'-phosphate was proposed to catalyze C–O cleavage in glucose 1-phosphate through protonation of a nonbridging oxygen.¹⁰⁴ A single protonation would have a small effect on the rate of C–O bond cleavage, though it would help ensure C–O rather than O–P cleavage. It is difficult to identify a potential general acid catalyst, partly because the position of phosphate varies significantly between structures. However, in

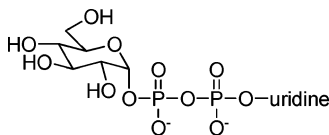
(92) The Pauling bond order, n_{ij} , between atoms i and j is calculated as $n_{ij} = e^{(r_1 - r_{ij})/0.3}$, where r_1 is the length of a single bond between atoms i and j , and r_{ij} is the length of the bond in question: $r_1(O-P) = 1.61 \text{ \AA}$, $r_1(C-O) = 1.41 \text{ \AA}$.

- (93) Schonbrunn, E.; Eschenburg, S.; Shuttleworth, W. E.; Schloss, J. V.; Amrhein, N.; Evans, J. N. S.; Kabsch, W. *Proc. Natl. Acad. Sci. U.S.A.* **2001**, *98*, 1376–1380.
 (94) Eschenburg, S.; Kabsch, W.; Healy, M. L.; Schonbrunn, E. *J. Biol. Chem.* **2003**, *278*, 49215–49222.
 (95) Park, H.; Hilsenbeck, J. L.; Kim, H. J.; Shuttleworth, W. A.; Park, Y. H.; Evans, J. N.; Kang, C. *Mol. Microbiol.* **2004**, *51*, 963–971.
 (96) Eschenburg, S.; Priestman, M.; Schonbrunn, E. *J. Biol. Chem.* **2005**, *280*, 3757–3763.
 (97) Huynh, Q. K.; Kishore, G. M.; Bild, G. S. *J. Biol. Chem.* **1988**, *263*, 735–739.
 (98) Dewel, H. S.; Radaev, S.; Wang, J.; Woodard, R. W.; Gatti, D. L. *J. Biol. Chem.* **2001**, *276*, 8393–8402.
 (99) Shumilin, I. A.; Bauerle, R.; Wu, J.; Woodard, R. W.; Kretsinger, R. H. *J. Mol. Biol.* **2004**, *341*, 455–466.
 (100) Gunawan, J.; Simard, D.; Gilbert, M.; Lovering, A. L.; Wakarchuk, W. W.; Tanner, M. E.; Strynadka, N. C. *J. Biol. Chem.* **2005**, *280*, 3555–3563.
 (101) Sprogøe, D.; van den Broek, L. A.; Mirza, O.; Kastrop, J. S.; Voragen, A. G.; Gajhede, M.; Skov, L. K. *Biochemistry* **2004**, *43*, 1156–1162.
 (102) Peapus, D. H.; Chiu, H.-J.; Campobasso, N.; Reddick, J. J.; Begley, T. P.; Ealick, S. E. *Biochemistry* **2001**, *40*, 10103–10114.
 (103) Zechel, D. L.; Withers, S. G. *Acc. Chem. Res.* **2000**, *33*, 11–18.
 (104) Jeremia, S.; Campagnolo, M.; Schinzel, R.; Johnson, L. N. *J. Mol. Biol.* **2002**, *322*, 413–423.

a structure containing glucose 1-phosphate, a water bridging to the phosphate of pyridoxal 5'-phosphate could potentially act as a general acid catalyst if that contact is retained in structures containing the second substrate, maltodextrin (PDB code: 1L5V).¹⁰⁴

B. Interactions through Nonbridging Oxygens. The same structures provide less compelling evidence for protonation of nonbridging oxygens. In AroA, Lys411 and Asp49 (through a bridging water) made contact with nonbridging oxygens, but Lys411 is not conserved and partitioning analysis showed that neither residue promotes phosphate departure.⁵³ There were no potentially catalytic residues within 4 Å of the nonbridging oxygens in KDO8P and DAHP synthases aside from the Lys residue that was also in contact with the bridging oxygen. In NeuB, Mn²⁺ was within 2.1 Å of a nonbridging oxygen, and two side chains contacting the bridging oxygen also made longer contacts with nonbridging oxygens, Lys129 at 3.2 Å and Glu234 at 3.9 Å. The sucrose phosphorylase structure did not contain phosphate, so it was not possible to identify nonbridging contacts. In thiamin phosphate synthase there was a single contact between a nonbridging oxygen and Mg²⁺. The maltodextrin phosphorylase structure was ambiguous. There were no good contacts beyond that described above for glucose 1-phosphate, but a phosphate-containing structure (PDB: 1L6I) formed good contacts with Lys574, 2.7 Å, and Tyr575, 3.3 Å. Thus, catalysis by diprotonation of nonbridging oxygens can be ruled out for AroA and MurA, KDO8P and DAHP synthase, and thiamin phosphate synthase. Residues that could potentially diprotonate phosphates appear to exist in NeuB, though they make closer contacts with the bridging oxygen, and in maltodextrin phosphorylase.

Applicability to Other Phosphate Esters. Phosphate diesters and triesters react through more associative mechanisms than monoesters, so the applicability of the findings from this study remain to be demonstrated. The reactivity of UDP-glucose (2) under acidic conditions was quite similar to glucose 1-phosphate, including giving predominantly C–O bond cleavage at low pH,¹⁰⁵ suggesting that the results of this study may be applicable at least to pyrophosphate phosphodiester compounds similar to UDP-glucose, including the pyrophosphates of the isoprenoid biosynthetic pathways.¹⁰⁶



2

Conclusions

The questions posed at the beginning of this study included: (1) Why does nonbridging oxygen protonation not affect the rate of THI breakdown? The results presented here demonstrate that while C–O bond lengths increase and ΔH_{C-O} 's decrease upon protonation of nonbridging oxygens, making the C–O bond more prone to cleavage, this is precisely offset by a decrease in proton affinity (read basicity, in solution) of the bridging oxygen, leading to no net effect on rate. Alternatively, if the ratio of equilibrium constants, K_{a1}/K_{a2} , equals the ratio of rate constants, a linear pH profile will be obtained. (2) What catalytic strategies are effective for C–O and O–P cleavage? Protonating the bridging oxygen is effective for promoting both C–O and P–O bond cleavage. Protonating nonbridging oxygens could promote C–O cleavage, but enzymes would have to diprotonate the phosphate to achieve a significant catalytic enhancement. (3) What factors control the choice between C–O and O–P cleavage, and how can enzymes influence that? The choice is controlled by the protonation state of the nonbridging oxygens and the nature of the organosubstituent. More protonation favors C–O bond cleavage. Organosubstituents that can form more stable cations also favor C–O bond cleavage. The answer to question number 1 demonstrates that enzymatic protonation of nonbridging oxygens would not necessarily increase the rate of C–O bond cleavage, but it would be useful for ensuring C–O versus O–P bond cleavage in reactants that are susceptible to both bonds breaking, such as glucose 1-phosphate. Conversely, not protonating the nonbridging oxygens would favor O–P bond cleavage in cases, such as dephosphorylation of Thr (of which *i*Pr–O–P_i is an analogue) by protein phosphatases, where either bond could break.

Acknowledgment. This work was supported by the Canadian Institutes of Health Research. We thank Prof. Paul Ayers (McMaster Chemistry) for invaluable discussions and advice on computational aspects of this study.

Supporting Information Available: Complete citation for ref 55, figures of Pauling bond orders, results of calculations using alternate computational methods, electron density at bond critical points, charge products (q_1q_2), guanidinium-containing structure, tables of bond lengths and bond orders, heterolytic bond dissociation energies, coordinates of optimized structures. This material is available free of charge via the Internet at <http://pubs.acs.org>.

JA057435C

(105) Bedford, C. T.; Hickman, A. D.; Logan, C. J. *Bioorg. Med. Chem.* **2003**, *11*, 2339–2345.

(106) Tidd, B. K. *J. Chem. Soc. B* **1971**, 1168–1176.